Journal of Computational Mathematics
Vol.28, No.2, 2010, 195–217.

http://www.global-sci.org/jcm
doi:10.4208/jcm.2009.10-m1004

CHEBYSHEV METHODS WITH DISCRETE NOISE: THE τ-ROCK METHODS*

Assyr Abdulle
Mathematics Section, Ecole Polytechnique Fédérale de Lausanne, CH-1015 Lausanne, Switzerland
Email: assyr.abdulle@epfl.ch
Yucheng Hu and Tiejun Li
Laboratory of Mathematics and Applied Mathematics and School of Mathematical Sciences, Peking University, Beijing 100871, China
Email: huyc@pku.edu.cn, tieli@pku.edu.cn

Abstract

Stabilized or Chebyshev explicit methods have been widely used in the past to solve stiff ordinary differential equations. Making use of special properties of Chebyshev-like polynomials, these methods have favorable stability properties compared to standard explicit methods while remaining explicit. A new class of such methods, called ROCK, introduced in [Numer. Math., 90, 1-18, 2001] has recently been extended to stiff stochastic differential equations under the name S-ROCK [C. R. Acad. Sci. Paris, 345(10), 2007 and Commun. Math. Sci, 6(4), 2008]. In this paper we discuss the extension of the S-ROCK methods to systems with discrete noise and propose a new class of methods for such problems, the τ-ROCK methods. One motivation for such methods is the simulation of multi-scale or stiff chemical kinetic systems and such systems are the focus of this paper, but our new methods could potentially be interesting for other stiff systems with discrete noise. Two versions of the τ-ROCK methods are discussed and their stability behavior is analyzed on a test problem. Compared to the τ-leaping method, a significant speed-up can be achieved for some stiff kinetic systems. The behavior of the proposed methods are tested on several numerical experiments.

Mathematics subject classification: 60G55; 65C30; 80A30
Key words: Stiff stochastic differential equations; Runge-Kutta Chebyshev methods; Chemical reaction systems; tau-leaping method

1. Introduction

The kinetic modeling of many complex chemical processes often involves reactions over a wide range of time scale and multiple chemical species with a very heterogeneous population size. Such processes arise for example in reaction and diffusion mechanisms in living cells, where the traditional modeling of the chemical reactions based on ordinary differential equations (ODEs) fails to capture the correct dynamics [1–3]. Indeed, when a small number of molecules are involved in a reaction, the stochasticity of the molecular collisions and the discreet behavior of the dynamics cannot be neglected.

Using first principle physical arguments (assuming proper mixing and thermal equilibrium) one can derive a discrete dynamics in the form of a Markov process with its accompanying master equation for the transition probability. Computing trajectories reproducing the statistics

* Received March 14, 2009 / Revised version received May 22, 2009 / Accepted June 6, 2009 / Published online December 21, 2009 /

of this master equation is at the heart of the so-called stochastic simulation algorithm (SSA) introduced by Gillespie in the late seventies [4,5]. Several coarse-graining procedure linking the Markov description to the ODE description of a chemical kinetic system have been derived. By lumping together several reactions in the SSA before updating the state vector one obtains a coarse-grained algorithm, known under the name of τ-leaping [6]. Coarse graining further leads to the so-called chemical Langevin equation (CLE), a system of stochastic differential equations (SDEs) and finally, neglecting the fluctuations through large volume approximation leads to the reaction rate equations, a system of ordinary differential equations.

The choice of the model and in turn of the algorithm, to describe and solve the chemical kinetic system is dictated by the specific properties of the considered system. A small number of molecules makes for example a description based on concentration unrealistic and would lead to favor a discrete description. But a discrete algorithm as SSA can be very expensive when many reactions occur leading to a huge number of updates of the state vector. Both the τ-leaping method and the Chemical Langevin description are good compromises between the SSA and the ODE model and have attracted increasingly growing attention.

A common issue for all of the above algorithms is the wide range of temporal scales of the chemical kinetic system. This multiscale nature is called stiffness in the ODE setting and numerical methods for stiff ODEs have been extensively studied [7]. Roughly speaking, stiffness in the ODE context leads to stability issues for traditional explicit methods (as the well-known forward-Euler method). The usual remedy to that problem is to use implicit methods which have favorable stability properties. But this comes with a cost, the cost of solving nonlinear problems at each time-step. An intermediate approach, between classical explicit methods and implicit methods, is known under the name of Chebyshev methods. These methods are explicit, but possess extended stability domains for dissipative problems. The extended stability domains can be tuned by varying the stage number of the methods [8–11]. A class of such Chebyshev methods, called ROCK (for Orthogonal Runge-Kutta Chebyshev) introduced in [8, 9], has recently be extended to stiff stochastic differential equations [12–14]. Mainly developed for problem arising from the method of lines discretization of stochastic partial differential equations (SPDE) [12, 13], these methods have proved successful for solving certain type of SDEs arising from CLE [14].

In this paper we further extend the (multi-stage) S-ROCK methods for discrete stochastic processes and derive several algorithms for processes with discrete Poisson noise. We study the application of such methods to discrete stochastic processes modeling chemical reactions usually solved by the so-called τ-leaping method. As explained above, the idea of lumping together several reactions in the SSA and updating the state space vector after a lumped time τ, led Gillespie to introduce the (explicit) τ-leaping method. It was soon recognized that in many situations, the timestep τ is dictated by the fastest reaction and can be prohibitively small. This triggered the development of other numerical schemes as the implicit τ-leaping methods [15]. But unlike stiff ODEs, stability is not the only issue for stochastic problems. Recovering the correct statistics of the stochastic process is not necessarily guaranteed by stable method. This has been discussed in [16] for SDEs and in [17] for the τ-leaping method. Roughly speaking, if a fast process of a dynamical system has a non trivial (e.g., non Dirac) invariant measure, explicit or implicit methods fail to capture the correct statistics unless the fast process is resolved. The damping properties of implicit methods and the amplification properties of explicit methods prevent to capture correctly these statistics [1)] . To overcome this

[1)] A particular algorithm, the so-called trapezoidal rule, is capable of recovering the limit behavior of a fast

issue, an adaptive explicit-implicit τ-leaping method has been introduced in [18]. Alternatively, multiscale techniques [20,21] aiming at capturing the slow (macro) process of a chemical kinetic system have been developed. Our new algorithm, the τ-ROCK methods, can be seen as a generalization of the explicit τ-leaping method and an explicit alternative of the explicit-implicit τ-leaping method. If restricted to one-stage, we recover the explicit τ-leaping method. Similarly as the S-ROCK methods, τ-ROCK methods are explicit and by increasing the stage number of the methods, we can increase their stability properties. By varying another parameter, the so-called damping parameter, we can vary the damping of the fastest scales.

We study several classes of chemical kinetic systems. The first-class, has similar dynamical properties as systems which are called mean-square stable in the theory of SDEs. For this class of problems, the τ-ROCK method show significant improvement compared to the explicit τ-leaping method. The second class of problems arise from reversible isomerization. The damping (or lack of damping) of the implicit or explicit τ-leaping methods reduce or increases the variance of the numerical solution. By tuning the damping of the τ-ROCK method, we show that we can obtain a more efficient method than the explicit τ-leaping method. The capability of the τ-ROCK method to be tuned for various situation makes this method attractive. But some issues are not yet fully addressed and need further developments. The tuning of our new method to the various scenarios is done by hand. An adaptive version, where the stage number, step-size and damping parameters can vary according to the behavior of the chemical kinetic system is currently under investigation.

This paper is organized as follows. In Sec. 2 we briefly review the SSA method, the τ-leaping method, and the Chebyshev and ROCK methods. In Sec. 3 we introduce several versions of the τ-ROCK methods corresponding to various treatments of the noise term. In Sec. 4 we study the convergence and stability properties of the τ-ROCK methods for the isomerization test equation. Finally, in Sec. 5 we present several numerical experiments to illustrate the behavior of the new methods.

2. SSA and τ-leaping

Assume that a well-stirred chemical reaction system has N chemical species $\{S_1, \ldots, S_N\}$ interacting through M reaction channels $\{R_1, \ldots, R_M\}$. The state of the system is specified by the vector $\boldsymbol{X}_t = (X_{1t}, \ldots, X_{Nt})^T$, where X_{it} denotes the number of molecules for the specie S_i at time t. Each reaction R_j is characterized by its propensity function $a_j(\boldsymbol{x})$ and its state-change vector $\boldsymbol{\nu}_j = (\nu_{1j}, \ldots, \nu_{Nj})^T$ $(j = 1, \ldots, M)$. The propensity function $a_j(x)$ gives the "stochastic rates" of the reaction channel j and involves the product of the number of molecules participating in the given reaction, while the state-change vector $\boldsymbol{\nu_j}$ is a integer valued vector describing the change of the state $\boldsymbol{X}_t$ when the reaction j fires (see [4,5]). In what follows, we denote the vector of the propensity functions as $\boldsymbol{a}(\boldsymbol{x}) = (a_1(\boldsymbol{x}), \ldots, a_M(\boldsymbol{x}))^T$, and the stoichiometry matrix as $\boldsymbol{\nu} = (\boldsymbol{\nu}_1, \ldots, \boldsymbol{\nu}_M)$. The rules governing the change in the species populations is given by the following stochastic evolution system.

1. Given the current state $\boldsymbol{X}_t$, during an infinitesimal time interval dt, the reaction R_j will fire with probability of $a_j(\boldsymbol{X}_t)dt$, and the reactions are independent of each other.

2. If R_j fires, the state of the system is updated as $\boldsymbol{X}_t + \boldsymbol{\nu}_j$.

process without resolving the fastest scale, but this characteristic seems to be limited to linear problems [16].

An exact simulation method for the above chemical kinetic system is the stochastic simulation algorithm [4, 5]. This method can be summarized as follows.

Algorithm 2.1 Stochastic simulation algorithm (SSA).

Step 1 Sample the waiting time τ as an exponentially distributed random variable with rate $a_0(\boldsymbol{X}_t) = \sum_{j=1}^{M} a_j(\boldsymbol{X}_t)$;

Step 2 Sample an M point random variable k with probability $a_j(\boldsymbol{X}_t)/a_0(\boldsymbol{X}_t)$ for the j-th reaction;

Step 3 Update $\boldsymbol{X}_{t+\tau} = \boldsymbol{X}_t + \boldsymbol{\nu}_k$ and return to Step 1.

Despite its simplicity and accuracy, the SSA is extremely slow for realistic simulations when the reactions fire very frequently. Instead of updating one reaction at a time, one could also fix a time-step τ and count all the reaction firing in this given interval. This lead to an approximate but much faster simulation procedure, the τ-leaping algorithm [6].

Algorithm 2.2 τ-leaping algorithm.

Step 1 Given the state $\boldsymbol{X}_n$ at time t_n, determine a leap time τ;

Step 2 Generate $\boldsymbol{r} = (r_1, \ldots, r_M)^T$, where $r_j = \mathcal{P}(a_j(\boldsymbol{X}_n)\tau)$ are Poisson random variables with rate $a_j(\boldsymbol{X}_n)\tau$;

Step 3 Update time to $t_n + \tau$ and $\boldsymbol{X}_{n+1} = \boldsymbol{X}_n + \boldsymbol{\nu} \cdot \boldsymbol{r}$.

For such an approximation of the SSA to be valid, τ should be chosen small enough so that in $(t, t+\tau]$ the propensity functions $a_j(\boldsymbol{X}_t)$ do not change appreciably [6] (this is called the *leap condition*). Strategy to choose the value of τ automatically and adaptively have been addressed by a few authors (see [18] and the references therein).

It was pointed out in [22] that the chemical kinetic system can be described by SDEs driven by state-dependent discrete Poisson noise. A rigorous description involving Poisson random measures is described in [22]. With a less-rigorous but more transparent statement, we may denote the SDE form of the chemical kinetic system as

$$d\boldsymbol{X}_t = \sum_{j=1}^{M} \boldsymbol{\nu}_j \mathcal{P}(a_j(\boldsymbol{X}_{t-})dt).$$

Actually, the τ-leaping method is just the forward-Euler scheme for this SDE:

$$\boldsymbol{X}_{n+1} = \boldsymbol{X}_n + \sum_{j=1}^{M} \boldsymbol{\nu}_j \mathcal{P}(a_j(\boldsymbol{X}_n)\tau) = \boldsymbol{X}_n + \boldsymbol{\nu} \cdot \boldsymbol{r}.$$

Now we make the decomposition

$$\begin{aligned} d\boldsymbol{X}_t &= \sum_{j=1}^{M} \boldsymbol{\nu}_j a_j(\boldsymbol{X}_{t-})dt + \sum_{j=1}^{M} \boldsymbol{\nu}_j \Big(\mathcal{P}(a_j(\boldsymbol{X}_{t-})dt) - a_j(\boldsymbol{X}_{t-})dt \Big) \\ &= \boldsymbol{f}(\boldsymbol{X}_{t-})dt + d\boldsymbol{Q}_t. \end{aligned} \tag{2.1}$$

Here

$$\boldsymbol{f}(\boldsymbol{x}) = \sum_{j=1}^{M} \boldsymbol{\nu}_j a_j(\boldsymbol{x})$$

and

$$d\boldsymbol{Q}_t = \sum_{j=1}^{M} \boldsymbol{\nu}_j \Big(\mathcal{P}(a_j(\boldsymbol{X}_{t-})dt) - a_j(\boldsymbol{X}_{t-})dt \Big)$$

are called the drift part and jump part in [22], respectively. This form is similar with SDEs driven by Brownian noise, except for the different noise.

The issue of stiffness. In chemical reaction systems, stiffness is a quite common phenomenon. For stiff SDEs, the forward-Euler scheme will suffer from stability issues. Similar issues arise for the τ-leaping method when solving stiff chemical kinetic systems. One possible remedy to this problem is to use a semi-implicit method to approximate (2.1), which was reported by M. Rathinam et al. in [15].

Algorithm 2.3 Implicit-τ-leaping algorithm.

Step 1 Given the state $\boldsymbol{X}_n$ at time t_n, determine a leap time τ;

Step 2 Generate Poisson random variables $\mathcal{P}(a_j(\boldsymbol{X}_n)\tau), j = 1, 2, \cdots, M$ and use them to compute

$$\boldsymbol{Q}(\boldsymbol{X}_n, \tau) = \sum_{j=1}^{M} \boldsymbol{\nu}_j \Big(\mathcal{P}(a_j(\boldsymbol{X}_n)\tau) - a_j(\boldsymbol{X}_n)\tau \Big)$$

Step 3 Solve the implicit equation

$$\boldsymbol{X}_{n+1} = \boldsymbol{X}_n + \boldsymbol{f}(\boldsymbol{X}_{n+1})\tau + \boldsymbol{Q}(\boldsymbol{X}_n, \tau).$$

As pointed out in [15], although attractive for some chemical kinetic systems, the damping property of the above implicit method prevent to capture the right statistics for several chemical kinetic systems with multiple time scales. An alternative algorithm also proposed in [15], the so-called trapezoidal τ-leaping algorithm shows better behavior for linear problems due to the fact, well-known in numerical ODE theory, that the trapezoidal rule has no "damping property at infinity" [7]. For the general case, an algorithm combining explicit and implicit τ-leaping method has been investigated in [18].

Remark 2.1. The τ-leaping method as the τ-ROCK methods that will be proposed in the following, have the property that the state change $\boldsymbol{X}_{n+1} - \boldsymbol{X}_n$ is generally not an integer vector. Rounding every component of $\boldsymbol{X}_n$ to their nearest integer is a simple remedy. Here, for simplicity in our numerical experiments, we will follow [15] and focus on the "unrounded" form. Another issue is that the component of $\boldsymbol{X}$ may become negative because of the unboundedness of the Poisson random variables. Negativity problem is more likely to happen for species with small population (as for example the species X_3 in the example 1 of Section 5). Our remedy is to take the absolute value of X if it becomes negative. One should be careful about this trick since it may bias some systems, but for the simple examples considered in this article this seems not to be an issue. We note that a τ-ROCK method based on binomial random variable could

be derived following the ideas developed below. The boundedness of theses random variable could be used to avoid negative population [19].

3. The τ-ROCK and Reversed-τ-ROCK Methods

The new methods that will be tested in this article are based on Chebyshev methods originally proposed for stiff ODEs and introduced by Saul'ev, Franklin & Guillou and Lago (see [7] and the references therein). Such methods rely on stability functions given by shifted Chebyshev-like polynomials $R_m(z) = T_m(1 + z/m^2)$, where $T_m(z)$ is the Chebyshev polynomial of degree m. The polynomials $R_m(z)$ (the stability functions of the underlying numerical methods) equi-oscillate between -1 and 1 and have the property that $|R_m(z)| \leq 1$ for $z \in [0, 2m^2]$. The related stability domains are therefore extended along the negative real axis and they increase *quadratically* with the degree m of $R_m(z)$. The degree m of the stability functions indicates the stage number of the associated Runge-Kutta method, while the property $R_m(z) = 1 + z + \mathcal{O}(z^2)$ ensure the first order convergence of the numerical method. These methods, further developed and generalized to higher orders in [8–11] have proved to be very efficient for large stiff ODEs.

The Chebyshev methods was successfully generalized to SDE [12–14] under the name S-ROCK, for stochastic orthogonal Runge-Kutta Chebyshev methods. They can efficiently solve a class of stiff SDEs that are called mean-square stable. In this article, we will extend the S-ROCK methods to chemical kinetic system of the form (2.1), driven by discrete Poisson noises. Following [12–14], we propose the so-called τ-ROCK methods for the numerical solution of (2.1).

Algorithm 3.1 m-stage τ-ROCK method.

Step 1 Given the state $\boldsymbol{X}_n$ at time t_n, determine a leap time τ;

Step 2 Using a three-term recurrence relation compute $\boldsymbol{K}_m$ as

$$\begin{aligned}
\boldsymbol{K}_0 =& \boldsymbol{X}_n, \quad \boldsymbol{K}_1 = \boldsymbol{K}_0 + \tau \frac{\omega_1}{\omega_0} \boldsymbol{f}(\boldsymbol{K}_0), \\
\boldsymbol{K}_j =& 2\tau\omega_1 \frac{T_{j-1}(\omega_0)}{T_j(\omega_0)} \boldsymbol{f}(\boldsymbol{K}_{j-1}) + 2\omega_0 \frac{T_{j-1}(\omega_0)}{T_j(\omega_0)} \boldsymbol{K}_{j-1} - \frac{T_{j-2}(\omega_0)}{T_j(\omega_0)} \boldsymbol{K}_{j-2}, \\
& j = 2, \ldots, m-1, \\
\boldsymbol{K}_m =& 2\tau\omega_1 \frac{T_{m-1}(\omega_0)}{T_m(\omega_0)} \boldsymbol{f}(\boldsymbol{K}_{m-1}) + 2\omega_0 \frac{T_{m-1}(\omega_0)}{T_m(\omega_0)} \boldsymbol{K}_{m-1} - \frac{T_{m-2}(\omega_0)}{T_m(\omega_0)} \boldsymbol{K}_{m-2} \\
& + \sum_{j=1}^{M} \boldsymbol{\nu}_j \Big(\mathcal{P}(a_j(\boldsymbol{K}_{m-1})\tau) - a_j(\boldsymbol{K}_{m-1})\tau \Big);
\end{aligned} \tag{3.1}$$

Step 3 Update the time to $t_n + \tau$ and $\boldsymbol{X}_{n+1} = \boldsymbol{K}_m$.

In (3.1) $T_j(x)$ is the classical Chebyshev polynomial which satisfies the recurrence relation

$$\begin{aligned}
& T_0(x) = 1, \ T_1(x) = x, \\
& T_j(x) = 2xT_{j-1}(x) - T_{j-2}(x), \ \ j \geq 2,
\end{aligned}$$

$\omega_0 = 1 + \eta/m^2$, $\eta > 0$ is a preselected constant called the damping parameter and $\omega_1 = T_m(\omega_0)/T'_m(\omega_0)$. $\mathcal{P}(a_j(\boldsymbol{K}_{m-1})\tau)$ are independent Poisson random variables with parameters $a_j(\boldsymbol{K}_{m-1})\tau$.

The difference between the τ-ROCK and the S-ROCK methods is merely in the noise term: the Gaussian noise in the S-ROCK method is replaced by the discrete noise

$$\boldsymbol{Q}(\boldsymbol{K}_{m-1},\tau) = \sum_{j=1}^{M} \boldsymbol{\nu}_j \Big(\mathcal{P}(a_j(\boldsymbol{K}_{m-1})\tau) - a_j(\boldsymbol{K}_{m-1})\tau\Big)$$

in the τ-ROCK method. Here

$$\tilde{N}_j(\boldsymbol{K}_{m-1},\tau) \equiv \Big(\mathcal{P}(a_j(\boldsymbol{K}_{m-1})\tau) - a_j(\boldsymbol{K}_{m-1})\tau\Big)$$

is the compensated-Poisson random variables satisfying

$$\mathbb{E}\tilde{N}_j(\boldsymbol{K}_{m-1},\tau) = 0,$$

and

$$\mathrm{Var}\tilde{N}_j(\boldsymbol{K}_{m-1},\tau) = a_j(\boldsymbol{K}_{m-1})\tau.$$

The τ-ROCK method can be viewed as a generalization of the τ-leaping method: in the case of $m = 1$, the τ-ROCK is exactly the τ-leaping. m can be chosen from one to several hundreds depending on the stiffness of the system. The advantage of using large m is that the quadratic growth of the stability domain along the negative real axis (suitable for stiff ODEs or SDEs) also enhance the stability properties of the ROCK version for discrete noise (as will be discussed in Section 4). However, as we mentioned before, stability is not the only concern in simulating stochastic processes. Like other explicit methods such as the τ-leaping method, the τ-ROCK methods also amplify the variance, sometimes even more severely as we aim at using large τ in our method. An alternative treatment of the noise term can damp this too large variance. The idea is to put the noise term at the beginning of the $m-$stage process. This "reversed" τ-ROCK method is given by the following process.

Algorithm 3.2 m-stage reversed-τ-ROCK method.

Step 1 Given the state $\boldsymbol{X}_n$ at time t_n, determine a leap time τ;

Step 2 Compute the noise term

$$\boldsymbol{Q}(\boldsymbol{X}_n,\tau) = \sum_{j=1}^{M} \boldsymbol{\nu}_j \left(\mathcal{P}(a_j(\boldsymbol{X}_n)\tau) - a_j(\boldsymbol{X}_n)\tau\right),$$

with $\boldsymbol{X}_n$ first, and then compute $\boldsymbol{K}_m$ iteratively as

$$\begin{aligned}
&\boldsymbol{K}_0 = \boldsymbol{X}_n + \boldsymbol{Q}(\boldsymbol{X}_n,\tau), \quad \boldsymbol{K}_1 = \boldsymbol{K}_0 + \tau\frac{\omega_1}{\omega_0}\boldsymbol{f}(\boldsymbol{K}_0),\\
&\boldsymbol{K}_j = 2\tau\omega_1\frac{T_{j-1}(\omega_0)}{T_j(\omega_0)}\boldsymbol{f}(\boldsymbol{K}_{j-1}) + 2\omega_0\frac{T_{j-1}(\omega_0)}{T_j(\omega_0)}\boldsymbol{K}_{j-1} - \frac{T_{j-2}(\omega_0)}{T_j(\omega_0)}\boldsymbol{K}_{j-2},\\
&\qquad j = 2,\ldots,m.
\end{aligned} \tag{3.2}$$

Step 3 Update time to $t_n + \tau$ and $\boldsymbol{X}_{n+1} = \boldsymbol{K}_m$.

This treatment of the noise term share some similarity with the implicit-τ-leaping method, where the noise term $\boldsymbol{Q}(\boldsymbol{X}_n, \tau)$ is added to $\boldsymbol{X}_n$ (but in this latter case, an implicit equation has to be solved for $\boldsymbol{X}_{n+1}$ while here, the *explicit* Chebyshev iterations ensure favorable stability properties for the above reversed-τ-ROCK method). It was shown in [17] that the implicit-τ-leaping method has damping properties and that the variance of $\boldsymbol{X}_n$ is reduced. Later we will show that the reversed-τ-ROCK method has a similar behavior.

So far, we have not discussed the choice of the stage number m, of the time-step τ and the damping parameter η, which is crucial for the overall performance of the τ-ROCK methods. Here we will use the selection procedure for m and η developed in [12–14] based on optimal stability domains for the numerical method when applied to linear scalar mean-square stable SDEs. For stiff chemical kinetic systems for which the variances of the fast components approach zero as $t \to \infty$ the above procedure works fine. However, as we will be seen in the numerical tests of Sec. 5, for stiff chemical kinetic system whose fast components do not satisfy the above variance property, the variance of the noise term $\tilde{N}_j(\boldsymbol{X}_n, \tau)$ can be very large (recall also that we aim at selecting large τ in our method). In such case we must choose a larger damping in the τ-ROCK methods than predicted by the strategy given in [12–14]. Currently this tuning is done by hand and a more automatic adaptive procedure including the adaptive determination of τ will be developed in a future work.

4. Stability Analysis

The simplest model problem to be considered is

$$S \xrightarrow{\lambda} \emptyset. \tag{4.1}$$

For such a reaction we have $\mathbb{E}(X_\infty) = \mathbb{E}(X_\infty^2) = 0$. The chemical Langevin equation corresponding to the above test equation is

$$dX_t = -\lambda X_t dt + \sqrt{\lambda X_t} dW_t, \tag{4.2}$$

where W_t is a standard Wiener process. This trivial test problem belongs to the class of so-called mean-square stable problems [14]. This is a special case of the test problem considered below (with $c_2 = 0$) and the stability condition $|R_m(z)| < 1,\ z = \lambda\tau$ (see (4.10) below) for the τ-ROCK method ensure that the long term behavior is correctly captured.
Notice that if this problem represents a fast reaction in a chemical reaction, small step-sizes for the usual τ-leaping method will be required as the condition $|1 - \lambda\tau| < 1$ must be satisfied which represents a severe restriction if λ is large.

To understand why the new methods work for some other stiff chemical kinetic systems, let us consider a model problem, the reversible isomerization reaction proposed in [17]

$$S_1 \underset{c_2}{\overset{c_1}{\rightleftharpoons}} S_2, \tag{4.3}$$

which plays the role of "test equation" in the numerical solution of ODEs here.

For this reversible reaction system, we always have the conservation for the total number of molecules. Let us define $X_{1t} + X_{2t} = X^T$ and $c_1 + c_2 = \lambda$. Since the total number of molecules X^T is constant, we will only consider on species X_{1t} (and two reactions) denoted by X_t in what follows. The propensity functions for this this system are given by

$$a_1(x) = c_1 x, \quad a_2(x) = c_2(X^T - x). \tag{4.4}$$

We will assume the total rate $\lambda \gg 1$ to take into account the stiffness. Analytically the system (4.3) has a stationary state X_∞ which follows the binomial distribution $B(n,p)$, where $n = X^T$ and $p = c_2/\lambda$. This stationary distribution can be obtained by computing the stationary distribution of the CME. We thus have

$$\mathbb{E}X^* \equiv \mathbb{E}(X_\infty) = \frac{c_2 X^T}{\lambda}, \quad \mathrm{Var}(X^*) \equiv \mathrm{Var}(X_\infty) = \frac{c_1 c_2 X^T}{\lambda^2}. \tag{4.5}$$

Remark 4.1. The direct integration of the chemical master equation associated with the reaction (4.3) with respect to x and x^2 gives

$$\mathbb{E}X_t = \frac{c_2 X^T}{\lambda}(1 - e^{-\lambda t}) + e^{-\lambda t}\mathbb{E}X_0, \tag{4.6}$$

$$\mathrm{Var}(X_t) = \frac{c_1 c_2 X^T}{\lambda^2}(1 - e^{-2\lambda t}) + e^{-2\lambda t}\mathrm{Var}(X_0) + \frac{c_1 - c_2}{\lambda}(e^{-\lambda t} - e^{-2\lambda t})\left(\mathbb{E}X_0 - \frac{c_2 X^T}{\lambda}\right). \tag{4.7}$$

We see, as t goes to infinity, that the mean and the variance of X_t approaches the values (4.5) obtained for the CME.

To investigate the numerical stability of the new methods, we follow a procedure similar to [17]. Applying the τ-ROCK method to the test problem (4.3) gives a difference equation (indexed by n) for the mean and variance of the stochastic process.

Definition 4.1. *Let $\{\boldsymbol{X}_n\}_{n\geq 0}$ be the sequence obtained by τ-leaping method applied to the test problem* (4.3)*. We will say that the mean and the variance of $\{\boldsymbol{X}_n\}_{n\geq 0}$ are absolutely stable if and only if for each component X_{in}, $|\mathbb{E}(X_{in})|$ and $|\mathrm{Var}(X_{in})|$ are bounded for $n \to \infty$, respectively.*

In what follows we will need the following formulas for the conditional expectation, known as the "law of total variance"

$$\mathbb{E}X = \mathbb{E}(\mathbb{E}(X|Y)), \quad \mathrm{Var}(X) = \mathbb{E}(\mathrm{Var}(X|Y)) + \mathrm{Var}(\mathbb{E}(X|Y)), \tag{4.8}$$

where X and Y are two random variables.

4.1. Stability analysis for the τ-ROCK method

To study the stability behavior of the τ-ROCK method, we apply the method to the problem (4.3) with propensity functions given by (4.4). In order to simplify the derivation below, we define the following new variables

$$Y_n = X_n - \frac{c_2 X^T}{\lambda}, \quad \tilde{K}_j = K_j - \frac{c_2 X^T}{\lambda}, \quad \tilde{f}(y) = \lambda y, z = \lambda\tau, \tag{4.9}$$

where $\lambda = c_1 + c_2$. The main result of this subsection is contained in the following lemma.

Lemma 4.1 (Stability and numerical limit analysis of the τ-ROCK) *The mean and the variance of the τ-ROCK scheme (Algorithm* 3.1*) are absolutely stable if and only if*

$$|R_m(z)| \leq 1, \tag{4.10}$$

where $R_m(z)$ is given by

$$R_m(z) = \frac{T_m(\omega_0 - \omega_1 z)}{T_m(\omega_0)}. \tag{4.11}$$

Furthermore, we have for the limit

$$\lim_{n\to\infty} \mathbb{E}X_n = \mathbb{E}X^*, \quad \lim_{n\to\infty} \mathrm{Var}(X_n) = \frac{2z}{1 - R_m^2(z)} \mathrm{Var}(X^*), \tag{4.12}$$

where $\mathbb{E}X^*$ and $\mathrm{Var}(X^*)$ are given by (4.5).

Proof. Applying the τ-ROCK method (Algorithm 3) to (4.3) and using the notations (4.9) we obtain

$$\begin{aligned}
\tilde{K}_0 =& Y_n, \quad \tilde{K}_1 = Y_n + \tau \frac{\omega_1}{\omega_0} \tilde{f}(\tilde{K}_0), \\
\tilde{K}_j =& 2\tau\omega_1 \frac{T_{j-1}(\omega_0)}{T_j(\omega_0)} \tilde{f}(\tilde{K}_{j-1}) + 2\omega_0 \frac{T_{j-1}(\omega_0)}{T_j(\omega_0)} \tilde{K}_{j-1} - \frac{T_{j-2}(\omega_0)}{T_j(\omega_0)} \tilde{K}_{j-2}, \\
& j = 2, \ldots, m-1, \\
\tilde{K}_m =& 2\tau\omega_1 \frac{T_{m-1}(\omega_0)}{T_m(\omega_0)} \tilde{f}(\tilde{K}_{m-1}) + 2\omega_0 \frac{T_{m-1}(\omega_0)}{T_m(\omega_0)} \tilde{K}_{m-1} - \frac{T_{m-2}(\omega_0)}{T_m(\omega_0)} \tilde{K}_{m-2} \\
& - \tilde{N}_1(K_{m-1}, \tau) + \tilde{N}_2(K_{m-1}, \tau),
\end{aligned}$$

where $\tilde{N}_1(K_{m-1}, \tau)$ and $\tilde{N}_2(K_{m-1}, \tau)$ are compensated-Poisson random variables

$$\begin{aligned}
\tilde{N}_1(K_{m-1}, \tau) &= \mathcal{P}(c_1 K_{m-1}\tau) - c_1 K_{m-1}\tau, \\
\tilde{N}_2(K_{m-1}, \tau) &= \mathcal{P}(c_2 (X^T - K_{m-1})\tau) - c_2 (X^T - K_{m-1})\tau.
\end{aligned}$$

Using the three-term recurrence relation of the Chebyshev polynomials, we obtain

$$\tilde{K}_j = \frac{T_j(\omega_0 - \omega_1 z)}{T_j(\omega_0)} Y_n, \quad j = 0, 1, \ldots, m-1, \tag{4.13}$$

$$\tilde{K}_m = \frac{T_m(\omega_0 - \omega_1 z)}{T_m(\omega_0)} Y_n - \tilde{N}_1(K_{m-1}, \tau) + \tilde{N}_2(K_{m-1}, \tau). \tag{4.14}$$

We have

$$\begin{aligned}
&\mathbb{E}(\tilde{N}_1(K_{m-1}, \tau)|Y_n) = \mathbb{E}(\tilde{N}_2(K_{m-1}, \tau)|Y_n) = 0, \\
&\mathrm{Var}(\tilde{N}_1(K_{m-1}, \tau)|Y_n) = c_1 K_{m-1}\tau, \quad \mathrm{Var}(\tilde{N}_2(K_{m-1}, \tau)|Y_n) = c_2 (X^T - K_{m-1})\tau.
\end{aligned}$$

Using (4.14) and (4.9) we obtain

$$\begin{aligned}
\mathbb{E}X_{n+1} = \mathbb{E}K_m &= \frac{c_2 X^T}{\lambda} + \mathbb{E}\tilde{K}_m = \frac{c_2 X^T}{\lambda} + R_m(z)\mathbb{E}Y_n \\
&= R_m(z) \left(\mathbb{E}X_n - \frac{c_2 X^T}{\lambda} \right) + \frac{c_2 X^T}{\lambda},
\end{aligned} \tag{4.15}$$

where $R_m(z)$ is given by (4.11). Now if $|R_m(z)| \leq 1$, then the mean is absolutely stable and a simple calculation gives

$$\mathbb{E}X_{n+1} = \sum_{j=0}^{n} (1 - R_m(z)) R_m^j(z) c_2 X^T + R_m^n(z)\mathbb{E}X_0 \tag{4.16}$$

from which we obtain the first equality of (4.12).

We consider next the difference equation for the variance. We have

$$\begin{aligned}\mathrm{Var}(X_{n+1}) =& R_m^2(z)\mathrm{Var}(Y_n) + \mathbb{E}(\mathrm{Var}(\tilde{N}_1(K_{m-1},\tau)|Y_n)) \\ &+ \mathbb{E}(\mathrm{Var}(\tilde{N}_2(K_{m-1},\tau)|Y_n))\end{aligned} \tag{4.17}$$

by (4.8). For the last two terms, a direct calculation gives

$$\mathbb{E}(\mathrm{Var}(\tilde{N}_1(K_{m-1},\tau)|Y_n)) = \frac{c_1c_2X^T}{\lambda}\tau\Big(1 - R_{m-1}(z)\Big) + c_1\tau R_{m-1}(z)\mathbb{E}X_n, \tag{4.18}$$

$$\mathbb{E}(\mathrm{Var}(\tilde{N}_2(K_{m-1},\tau)|Y_n)) = \frac{c_1c_2X^T}{\lambda}\tau + \frac{c_2^2X^T}{\lambda}\tau R_{m-1}(z) - c_2\tau R_{m-1}(z)\mathbb{E}X_n. \tag{4.19}$$

Combining equations (4.17), (4.18) and (4.19), we obtain

$$\begin{aligned}\mathrm{Var}(X_{n+1}) =& R_m^2(z)\mathrm{Var}(X_n) + (c_1 - c_2)\tau R_{m-1}(z)\mathbb{E}X_n \\ &+ \frac{2c_1c_2X^T}{\lambda}\tau - \frac{(c_1 - c_2)c_2X^T}{\lambda}\tau R_{m-1}(z).\end{aligned} \tag{4.20}$$

Substituting (4.16) in the above equation, we obtain a difference equation for the variance. It can be seen that the variance is absolutely stable if $|R_m(z)| \le 1$ holds. Under this condition, one can solve this difference equation and we obtain the second equality of (4.12). □

Comparison with the (explicit) τ-leaping method. A similar stability analysis for the explicit τ-leaping method shows that the step-size (that we denote by τ_e for this method) must satisfy

$$|1 - \lambda\tau_e| \le 1$$

for the mean and the variance to be stable for the test problem (4.3). This restriction is the same as the usual restriction for the forward Euler method applied to the Dahlquist test problem $dy/dt = -\lambda y$ in ODE theory, namely

$$\tau_e \le \frac{2}{\lambda},$$

which is a severe restriction if λ is large. For the τ-ROCK method, taking advantage of the quadratic increase of the stability region along the real axis

$$|R_m(z)| \le 1 \quad \text{for } z \in [0, cst(\eta)\cdot m^2],$$

i.e.,

$$\tau \le \frac{cst(\eta)\cdot m^2}{\lambda}.$$

where $cst(\eta)$ is a decreasing function depending on η. Note that $cst(0) = 2$ and $\lim_{\eta\to\infty} cst(\eta) = 2/m$ [12,13]. In each time-step, the τ-ROCK method needs m times the number of propensity functions evaluation compared with the τ-leaping method while it needs *the same* number of random variable generation. We thus define the (theoretical) effective deterministic and stochastic time-step, $\tau_{eff,d}$ and $\tau_{eff,s}$, respectively by

$$\tau_{eff,d} = \frac{\tau}{m} = \frac{cst(\eta)\cdot m}{\lambda}, \quad \tau_{eff,s} = \frac{cst(\eta)\cdot m^2}{\lambda}, \tag{4.21}$$

and compared to the τ-leaping method, we have the following theoretical gain in efficiency

$$\tau_{eff,d} = \frac{cst(\eta)\cdot m}{2}\tau_e, \quad \tau_{eff,s} = \frac{cst(\eta)\cdot m^2}{2}\tau_e. \tag{4.22}$$

Numerical examples in Section 5 will show the practical gain in efficiency. As seen in the equation above, it depends on the damping coefficient η whose tuning will depend on the problem.

Remark 4.2. It is interesting to note that the stability condition (4.10) is formally the same as that of the ROCK methods for deterministic ODEs [8, 9], but different from the stability condition to ensure mean square stability for the S-ROCK methods (applied to stiff SDEs) [12–14]. Despite this formal similarity, the difference between stability properties of the the current scheme and the ROCK methods for ODEs is reflected in the variance term in (4.12). Usually, by selecting a large damping parameter η (see Section 3), we will obtain an amplifying factor such that $R_m(z) \ll 1$. As z is usually large for stiff systems, the results of the above lemma show that for τ-ROCK methods, the numerical variance will be enlarged. This phenomenon, due to the non-trivial invariant distribution for chemical kinetic systems as (4.3) was noted in [17] and well as in [16] for SDEs.

4.2. Stability analysis of the reversed-τ-ROCK method

Similar procedures as in the last subsection can be applied to the m-stage reversed-τ-ROCK scheme. We summarize the results in the following lemma.

Lemma 4.2 (Stability and numerical limit analysis of the reversed-τ-ROCK) *The mean and the variance of the reversed-τ-ROCK scheme* (*Algorithm* 3.2) *are absolutely stable if and only if*

$$|R_m(z)| \leq 1, \tag{4.23}$$

where the $R_m(z)$ is given by (4.11). *Furthermore, we have for the limit*

$$\lim_{n\to\infty} \mathbb{E}X_n = \mathbb{E}X^*, \quad \lim_{n\to\infty} \mathrm{Var}(X_n) = \frac{2zR_m^2(z)}{1-R_m^2(z)}\mathrm{Var}X^*, \tag{4.24}$$

where $\mathbb{E}X^*$ and $\mathrm{Var}(X^*)$ are given by (4.5).

Remark 4.3. Let us note the difference between the equations (4.12) and (4.24). To obtain the correct limit for the variance, one can adjust the amplifying factor $2zR_m^2(z)/(1-R_m^2(z))$ by choosing a suitable damping parameter η, which is analyzed in the next subsection.

Proof. Applying the modified τ-ROCK method (Algorithm 3) to (4.3) and using the notations (4.9) we obtain

$$\begin{aligned}
\tilde{K}_0 =& Y_n - \tilde{N}_1(X_n,\tau) + \tilde{N}_2(X_n,\tau),\\
\tilde{K}_1 =& \tilde{K}_0 + \tau\frac{\omega_1}{\omega_0}\tilde{f}(\tilde{K}_0),\\
\tilde{K}_j =& 2\tau\omega_1\frac{T_{j-1}(\omega_0)}{T_j(\omega_0)}\tilde{f}(\tilde{K}_{j-1}) + 2\omega_0\frac{T_{j-1}(\omega_0)}{T_j(\omega_0)}\tilde{K}_{j-1} - \frac{T_{j-2}(\omega_0)}{T_j(\omega_0)}\tilde{K}_{j-2},\\
& j = 2,\dots,m,
\end{aligned} \tag{4.25}$$

where

$$\begin{aligned}
\tilde{N}_1(X_n,\tau) &= \mathcal{P}(c_1X_n\tau) - c_1X_n\tau,\\
\tilde{N}_2(X_n,\tau) &= \mathcal{P}(c_2(X^T - X_n)\tau) - c_2(X^T - X_n)\tau.
\end{aligned} \tag{4.26}$$

Similarly as in the Lemma 4.1 we obtain

$$X_{n+1} - \frac{c_2 X^T}{\lambda} = Y_{n+1} = R_m(z)\left(Y_n - \tilde{N}_1(X_n,\tau) + \tilde{N}_2(X_n,\tau)\right). \tag{4.27}$$

For the mean, we obtain the same difference equation as for the τ-ROCK method

$$\begin{aligned}\mathbb{E}X_{n+1} = \mathbb{E}K_m &= \frac{c_2 X^T}{\lambda} + \mathbb{E}\tilde{K}_m = \frac{c_2 X^T}{\lambda} + R_m(z)\mathbb{E}Y_n \\ &= R_m(z)\left(\mathbb{E}X_n - \frac{c_2 X^T}{\lambda}\right) + \frac{c_2 X^T}{\lambda}.\end{aligned} \tag{4.28}$$

Hence, the absolute stability of the mean holds under the condition (4.23) and we have the first equality of (4.24). For the variance, we have

$$\mathrm{Var}(X_{n+1}) = R_m^2(z)\big(\mathrm{Var}(X_n) + (c_1 - c_2)\tau\mathbb{E}X_n + c_2\tau X^T\big).$$

The absolute stability of the variance is guaranteed if (4.23) and similar calculation as in Lemma 4.1 give the second equality of (4.24).

4.3. Damping effect in the reversed-τ-ROCK method

Consider (4.24) and define $\tilde{r}(m,\eta,z) = 2zR_m^2(z)/(1-R_m^2(z))$ to be the damping function of the reversed-τ-ROCK method. It depends on m, η and z. Define $D = [-l_\eta^m, 0]$ the (real) stability domain of R_m. With the assumption of a large damping, we have $R_m^2(z) \ll 1$ in the interior of the stability domain and we can study

$$r(m,\eta,z) = 2zR_m^2(z) = 2z\frac{T_m^2(\omega_0 - \omega_1 z)}{T_m^2(\omega_0)}. \tag{4.29}$$

We note that $T_m^2(\omega_0 - \omega_1 z)$ oscillates between 0 and 1 in D while the term $T_m^2(\omega_0)$ makes $R_m^2(z)$ oscillates between 0 and $1/T_m^2(\omega_0)$. Our goal is to control the amplification factor $r(m,\eta,z)$, say

$$\rho(m,\eta,z) = \frac{2z}{T_m(\omega_0)^2} = \alpha, \tag{4.30}$$

where α is not too large (note that $\eta = \eta(m,z)$). The following formula is well-known for Chebyshev polynomials

$$T_m(x) = \frac{(x+\sqrt{x^2-1})^m + (x-\sqrt{x^2-1})^m}{2} = \frac{I_1 + I_2}{2}.$$

For $x = \omega_0$, we have

$$I_1 = \omega_0^m\left(1 + \sqrt{1-\omega_0^{-2}}\right)^m,$$

and for $\omega_0 > 1$ and m large

$$T_m(\omega_0) \simeq \frac{\omega_0^m}{2}\left(1 + \sqrt{1-\omega_0^{-2}}\right)^m. \tag{4.31}$$

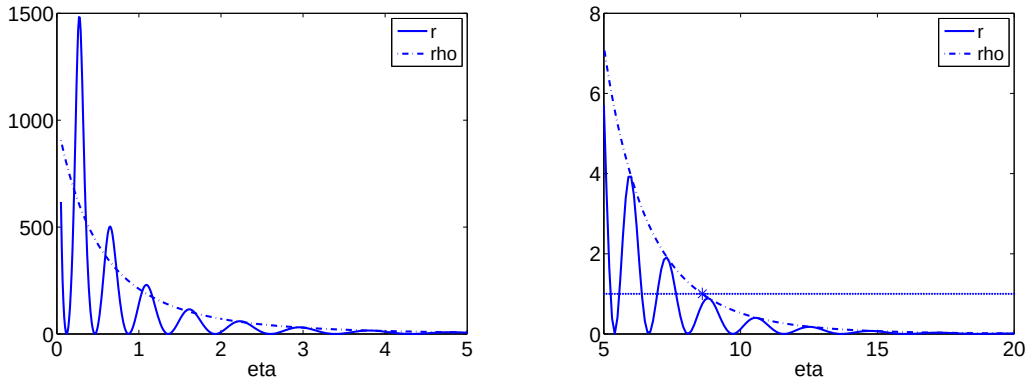

(a) $\eta \in (0, 5)$ (b) $\eta \in (5, 20)$

Fig. 4.1. Behavior of the damping coefficient r (solid line) and ρ (dashed line). The star symbol in the right plot corresponds to the η^* predicted by (4.32) with $\alpha = 1$. We can see the position of '*' is approximately at the intersection of ρ and the straight line $\alpha = 1$.

Using this approximation for $T_m(\omega_0)^2$ in (4.30) we have

$$\frac{\omega_0^{2m}}{4}\left(1+\sqrt{1-\omega_0^{-2}}\right)^{2m} = \frac{2z}{\alpha}$$

and after some calculations

$$\omega_0 = \frac{1+\beta^2}{2\beta},$$

where $\beta = (8z/\alpha)^{1/(2m)}$. Finally, as $\omega_0 = 1 + \eta/m^2$, we obtain

$$\eta = \frac{(1-\beta)^2}{2\beta}m^2. \tag{4.32}$$

Below is a numerical study of the damping functions r and ρ, defined in (4.29) and (4.30) respectively. We fix $m = 100$, $z = \lambda\tau = 2000 \times 0.25 = 500$ and let η vary. We can see in Fig. 4.1 that the oscillations of r are damped as η increases and the function ρ gives a reasonable bound for r for sufficient large η. We denote by η^* the value of η predicted by (4.32) for $\alpha = 1$. We can see in Fig. 4.1 that $r(m, \eta^*, z) \leq \rho(m, \eta^*, z) \approx \alpha = 1$. For some stiff chemical kinetic systems a smaller value for α is requested, in order to have a smaller damping function. Indeed, the noise term $\boldsymbol{Q}(\boldsymbol{X}_n, \tau)$ in the τ-ROCK method may become much larger than the real fluctuation of the system for large τ and we need smaller values of α say $\alpha = 0.01, 0.001$ in order to control the growth of the variance.

5. Numerical Experiments

In this section, we test our methods on some stiff chemical kinetic systems. Numerical results show that our methods correctly capture the mean with much larger time-steps than the τ-leaping method. We will also see that the τ-ROCK method usually amplifies the variances of the fast variables of the system, while the reversed-τ-ROCK method usually damps theses

variances. These numerical observations are in agreement with our theoretical analysis in Sec. 4. The amplifying or damping effects on the variances of the fast variables are not an issue for chemical systems with trivial invariant measure for the fast variables. This is the case in the Example 1 below. Indeed for such problems, the stability of the moments of the system is sufficient to capture the right effective slow process [14–16]. For this kind of systems, both the τ-ROCK and the reversed-τ-ROCK methods can use much larger effective step-size than the τ-leaping method.

However, when the fast variables of the chemical system have non-trivial invariant measures, the damping or amplifying effects of the variances of these variables will induce large errors in the effective system [14–16]. Such a system is studied in Example 2. We find in our numerical experiments that for linear propensity function (as studied in this example) the effective step-size of τ-ROCK and the reversed-τ-ROCK methods is still larger than the step-size needed for the τ-leaping method, although the variance of the fast variable is amplified (resp. damped) significantly. For non-linear propensity function, such as in Example 3, there seems to be no gain in the effective step-size of the new methods.

Finally, let us mention that besides using larger time-step, the new methods also needs much less random variable generations than the τ-leaping method. Indeed, we need only to draw the Poisson random variables once in each (large) time-step Δt. To illustrate this fact, we will also in what follows compare the number of random variable generation needed for the simulation of a chemical system.

5.1. Example 1

We consider the so-called Michaelis-Menten system describing the kinetics of many enzymes. The reaction involves four species: S_1 (a substrate), S_2 (an enzyme), S_3 (an enzyme-substrate complex) and S_4 (a product). It can be described as follows: the enzyme binds to the substrate to form an enzyme-substrate complex which is then transformed into the product or can dissociate back into enzyme and substrate i.e.,

$$\begin{aligned} S_1 + S_2 &\xrightarrow{c_1} S_3, \\ S_3 &\xrightarrow{c_2} S_1 + S_2, \\ S_3 &\xrightarrow{c_3} S_2 + S_4. \end{aligned}$$

The mathematical description of this process can be found in [23]. The state-change vectors are $\nu_1 = (-1,-1,1,0)^T$, $\nu_2 = (1,1,-1,0)^T$ and $\nu_3 = (0,1,-1,1)^T$. The propensity functions

Table 5.1: Comparison of the deterministic and the stochastic effective step-size needed for Example 1, using the τ-leaping and the τ-ROCK methods. We used the values $c_3 = 10, 100, 10^3$, and 10^4. The step-size for the τ-ROCK method is chosen as $\tau = 0.25$ and we denote by δt the step-size for the τ-leaping method.

	τ-leaping		τ-ROCK		
	δt	# of random variables	$\tau_{eff,d}$	$\tau_{eff,s}$	# of random variables
$c_3 = 10$	0.15	300	0.0833	0.25	180
$c_3 = 100$	0.05	9000	0.0313	0.25	180
$c_3 = 10^3$	10^{-5}	4.5×10^6	0.0086	0.25	180
$c_3 = 10^4$	2.5×10^{-6}	1.8×10^7	0.0024	0.25	180

Table 5.2: Mean of $\boldsymbol{X}$ at $t = 15$ in Example 1 (sample size $n = 10000$, $c_3 = 1000$).

	SSA	τ-ROCK	reversed-τ-ROCK
$X_1(15)$	151.0	150.1	150.2
$X_2(15)$	119.0	120.0	120.0
$X_3(15)$	1.0	0.04	0.03
$X_4(15)$	2848.0	2850.0	2849.8

Table 5.3: Sample standard deviation of $\boldsymbol{X}$ at $t = 15$ in Example 1 (sample size $n = 10000$, $c_3 = 1000$).

	SSA	τ-ROCK	reversed-τ-ROCK
$X_1(15)$	11.9	12.0	11.8
$X_2(15)$	0.2	3.9	0.05
$X_3(15)$	0.2	3.9	0.05
$X_4(15)$	12.0	12.1	11.8

are given by $a_1(\boldsymbol{x}) = c_1 x_1 x_2$, $a_2(\boldsymbol{x}) = c_2 x_3$ and $a_3(\boldsymbol{x}) = c_3 x_3$. The initial value and rate constants are set as $X_1(0) = 3000$, $X_2(0) = 120$, $X_3(0) = X_4(0) = 0$ and $c_1 = 1.66 \times 10^{-3}$, $c_2 = 10^{-4}$. c_3 is tuned to control the stiffness of the system. We simulate the system in the time interval $[0, 15]$.

To test the efficiency of the methods, we increase the value of c_3, corresponding to an increasingly fast production rate. The effective step-size and number of random variables needed in each simulation by using different methods are given in Table 5.1. We can see that as the system become stiff, the explicit-τ-leaping method become inefficient. For $c_3 = 1000$, the step-size reduction due to stiffness forces the explicit τ-leaping method to take step-size close to 10^{-5} in order to perform a stable integration and in turn to generate, for each trajectory, $(1.5 \times 10^6) \times 3 = 4.5 \times 10^6$ Poisson random variables (here the factor 3 comes from the three reactions of the system as each reaction needs one random variable generation for each step-size). In contrast, for the τ-ROCK or reversed-τ-ROCK methods, we can fix $\tau = 0.25$ and tune the stage number $m = 29$ and we only need to generate $60 \times 3 = 180$ Poisson random variables for each trajectory. Hence the (deterministic and stochastic) effective step-sizes (see (4.21)) are given by $\tau_{eff,d} = 0.25/29 = 0.0086$ and $\tau_{eff,s} = 0.25$. We see that, by taking advantage of the extended stability properties, the τ-ROCK and reversed-τ-ROCK methods are several order of magnitude more efficient compared with the explicit-τ-leaping method.

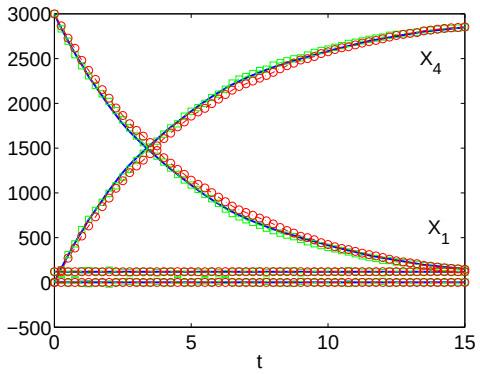

Fig. 5.1. A trajectory of Example 2 for $c_3 = 1000$ simulated by SSA (blue line), τ-ROCK (green square) and reversed-τ-ROCK (red circle) methods.

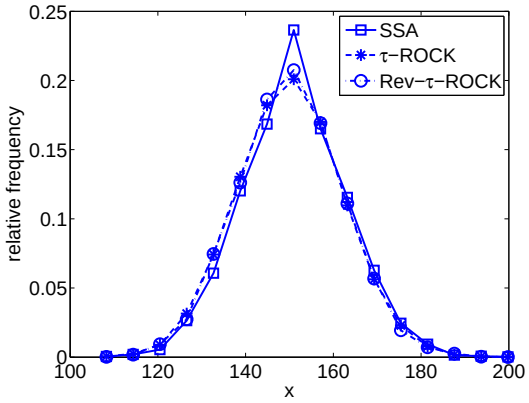

Fig. 5.2. Histogram (sample size $n = 10000$, $c_3 = 1000$) for X_1 at $t = 15$ in Example 1, computed by the SSA (solid-square), the τ-ROCK method (dashed-star) and the reversed-τ-ROCK method (dotted-circle).

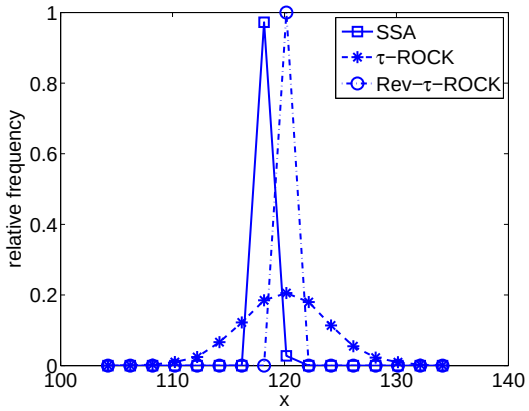

Fig. 5.3. Histogram (sample size $n = 10000$, $c_3 = 1000$) for X_2 at $t = 15$ in Example 1, computed by the SSA (solid-square), the τ-ROCK method (dashed-star) and the reversed-τ-ROCK method (dotted-circle).

Next we let $c_3 = 1000$ fixed and test the accuracy of the τ-ROCK and reversed-τ-ROCK methods by comparing them with the SSA. Fig. 5.1 depicts a trajectory of $\boldsymbol{X}$ simulated using the SSA, τ-ROCK and reversed-τ-ROCK. Table 5.2 and Table 5.3 give the mean and standard deviation of $X_1, \ldots, X_4$ at $t = 15$ for the different methods. From these results, we can see that for the slow variables X_1 and X_4 both the mean and variance are well-captured by the new methods; for the fast variable X_2 and X_3, however, the variances are amplified by the τ-ROCK method and damped by the reversed-τ-ROCK method. From the histograms of X_1 and X_2 at $t = 15$ in Fig. 5.2 and Fig. 5.3 it can also be seen that the statistics are well-captured for the slow variable X_1 (or X_4) but not for fast variable X_2 (or X_3).

For this system, the SDEs in the form of (2.1) can be written as

$$\begin{aligned}
dX_1 &= -c_1 X_1 X_2 dt + c_2 X_3 dt - \tilde{N}_1(\boldsymbol{X}, dt) + \tilde{N}_2(\boldsymbol{X}, dt),\\
dX_2 &= -c_1 X_1 X_2 dt + c_2 X_3 dt + c_3 X_3 dt - \tilde{N}_1(\boldsymbol{X}, dt) + \tilde{N}_2(\boldsymbol{X}, dt) + \tilde{N}_3(\boldsymbol{X}, dt),\\
dX_3 &= c_1 X_1 X_2 dt - c_2 X_3 - c_3 X_3 + \tilde{N}_1(\boldsymbol{X}, dt) - \tilde{N}_2(\boldsymbol{X}, dt) - \tilde{N}_3(\boldsymbol{X}, dt),\\
dX_4 &= c_3 X_3 dt + \tilde{N}_3(\boldsymbol{X}, dt).
\end{aligned} \tag{5.1}$$

The noises $\tilde{N}_j(\boldsymbol{X}, dt), j = 1, 2, 3$ are compensated Poisson random variables with mean equal to zero and variance $\mathrm{Var}(\tilde{N}_1(\boldsymbol{X}, dt)) = c_1 X_1 X_2 dt$, $\mathrm{Var}(\tilde{N}_2(\boldsymbol{X}, dt)) = c_2 X_3 dt$ and $\mathrm{Var}(\tilde{N}_3(\boldsymbol{X}, dt)) = c_3 X_3 dt$. The stiffness in this system come from the third equation. From the system (5.1) one can see that as c_3 increases, the value of X_3 will tend to the slow manifold at $X_3 = 0$ so that the product $c_3 X_3$ will remain small and the variance of the noise $\mathrm{Var}(\tilde{N}_3(\boldsymbol{X}, \tau))$ will approach zero as X_3 goes to zero. This behavior is related to the mean-square stability of SDEs discussed in [14].

5.2. Example 2

For our second example, we consider the chemical reaction system given by

$$S_1 \underset{c_2}{\overset{c_1}{\rightleftharpoons}} S_3,$$
$$S_1 + S_2 \xrightarrow{c_3} S_1 + S_4.$$

Observe that the total number of S_1 and S_3 molecules is constant (denoted by X^T), and if we do not care about the by-product S_4, the system can be described by two variables $\boldsymbol{X} = (X_1, X_2)$ (numbers of S_1 and S_2 molecules, respectively) and three reactions. The propensity functions are

$$a_1(\boldsymbol{x}) = c_1 x_1,$$
$$a_2(\boldsymbol{x}) = c_2(X^T - x_1),$$
$$a_3(\boldsymbol{x}) = c_3 x_1 x_2.$$

Following [15], we choose $c_1 = c_2 = 10^5$, $c_3 = 0.0005$, and $X^T = 20000$ and the initial conditions $\boldsymbol{X}(0) = (10000, 100)$. We solve the system in the time interval $[0, 0.01]$.

The reversible reaction is the fast reaction of this system. If we consider this reaction only, and denote X_1 as X and $c_1 = c_2 = \lambda/2$, then it is easy to verify that X satisfy the (Poisson noise driven) SDE (2.1) given by

$$dX = -\lambda X dt + \frac{\lambda}{2} X^T dt + \tilde{N}(X, dt), \tag{5.2}$$

where $\tilde{N}(X, dt)$ is a random variable with mean zero and variance equal to $\lambda X^T dt/2$. When $\lambda \gg 1$, the system becomes stiff and the deterministic part of (5.2) forces an explicit method (as the Euler method) to take a step-size τ whose size is dictated by the the fastest reaction

$$\lambda\tau < 2,$$

which is a severe restriction if $\lambda \gg 1$. Numerically, we find that as the step size approaches 1×10^{-5}, the explicit-τ-leaping method will become unstable.

Let us apply the new methods to that problem. We set the time-step to $\tau = 0.001$ and adapt the stage number and the damping parameter according to the procedure given in [14]. This gives $m = 26$ and $\eta = 20$, which is seen to give a stable integration. The effective step-size $\tau/m = 3.8 \times 10^{-5}$ is approximately 4 times larger than the step-size of the explicit-τ-leaping. Let us briefly discuss the random variable generation issue. With the explicit τ-leaping method, taking a step-size of 5×10^{-6} leads to the generation of$2000 \times 3 = 6000$ random variables for each simulation of a trajectory. For the new methods with $\tau = 0.001$, we only need to generate

$10 \times 3 = 30$ random variables for each simulation trajectory. There is thus a significant speed up for the new methods.

We now test the accuracy of the new methods for this system. Fig. 5.4 depicts sample trajectories of the fast variable X_1, simulated by the SSA, τ-ROCK and the reversed-τ-ROCK methods, respectively. Compared with the SSA, the τ-ROCK method predicts larger fluctuation for X_1, while the reversed-τ-ROCK method predicts smaller fluctuation for X_1, as can be seen in Table 5.5. This observation (consistent with our analysis of Section 4) seems to indicate that a suitable combination of the τ-ROCK and the reversed-τ-ROCK methods could lead to better capture the variance. This need further investigation and will be reported elsewhere. Table 5.4 shows that both methods capture adequately the mean of X_1 and X_2. For the slow variable X_2, the variance is also well captured. The histograms for X_1 and X_2, computed by the SSA, the τ-ROCK and the reversed-τ-ROCK methods, are given in Fig. 5.5 and Fig. 5.6, respectively.

From the numerical results of Example 2 (as well as from our theoretical analysis)

5.3. Example 3

Our last example is the decaying-dimerizing reaction equation studied in [6]. It consists of three species S_1, S_2, and S_3 and four reaction channels

$$\begin{aligned} S_1 &\xrightarrow{c_1} \emptyset, \\ S_1 + S_1 &\xrightarrow{c_2} S_2, \\ S_2 &\xrightarrow{c_3} S_1 + S_1, \\ S_2 &\xrightarrow{c_4} S_3. \end{aligned}$$

We choose the same values of the parameters as given in [15], that is, $c_1 = 1$, $c_2 = 10$, $c_3 = 1000$, and $c_4 = 0.1$. For the initial conditions, $X_1(0) = 400$, $X_2(0) = 798$, and $X_3(0) = 0$ were chosen in [15] to lie on the slow manifold

$$X_2 = \frac{5}{1000} X_1(X_1 - 1),$$

which is an approximate slow manifold for the above system. The propensity functions are given by $a_1(\boldsymbol{x}) = c_1 x_1$, $a_2(\boldsymbol{x}) = c_2 x_1(x_1 - 1)/2$, $a_3(\boldsymbol{x}) = c_3 x_2$, and $a_4(\boldsymbol{x}) = c_4 x_2$. The problem is solved on the time interval $[0, 0.2]$.

We plot in Fig. 5.7 a trajectory, computed with the SSA, of the decaying-dimerizing reactions. We see that X_1 a X_2 exhibit significant fluctuations due to the non-linear reversible reaction

$$2S_1 \underset{c_3}{\overset{c_2}{\rightleftharpoons}} S_2. \tag{5.3}$$

Table 5.4: Sample mean of $\boldsymbol{X}$ at $t = 0.01$ in Example 2 (sample size $n = 10000$).

	SSA	τ-ROCK	reversed-τ-ROCK
$X_1(0.01)$	10001.00	9987.90	9999.90
$X_2(0.01)$	95.00	95.13	95.11

Table 5.5: Sample standard deviation of $\boldsymbol{X}$ at $t = 0.01$ in Example 2 (sample size $n = 10000$).

	SSA	τ-ROCK	reversed-τ-ROCK
$X_1(0.01)$	72.95	1422.20	23.70
$X_2(0.01)$	2.22	2.18	2.19

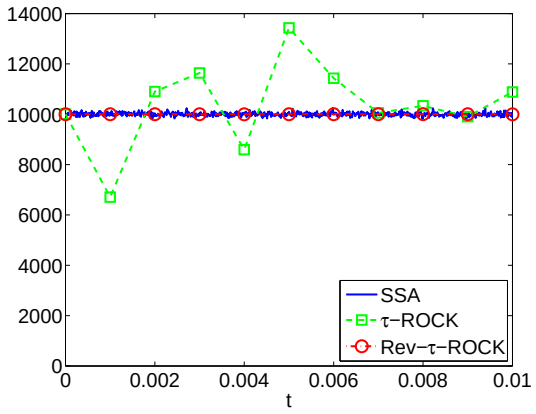

Fig. 5.4. A trajectory of X_1 for Example 2 simulated by SSA (blue line), τ-ROCK (green square) and reversed-τ-ROCK (red circle) methods.

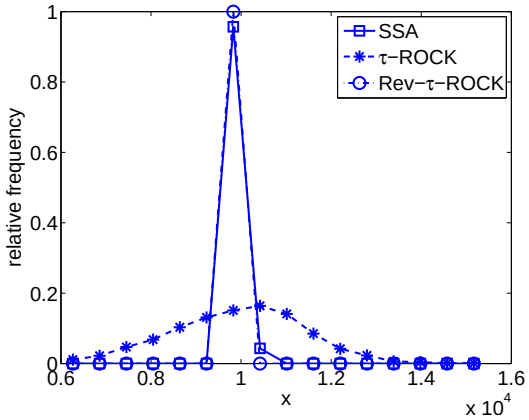

Fig. 5.5. Histogram (sample size $n = 10000$) for X_1 at $t = 0.01$ for Example 2 computed by the SSA (solid-square), the τ-ROCK method (dashed-star) and the reversed-τ-ROCK method (dotted-circle).

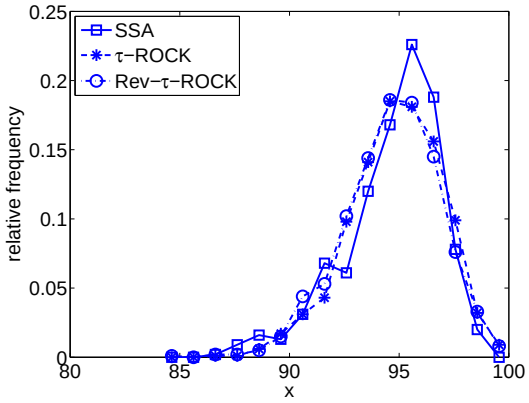

Fig. 5.6. Histogram (sample size $n = 10000$) for X_2 at $t = 0.01$ for Example 2 computed by the SSA (solid-square), the τ-ROCK method (dashed-star) and the reversed-τ-ROCK method (dotted-circle).

For simplicity we neglect the other two reactions and focus on the system (5.3). By the conservation law $X_1 + 2X_2 = X^T$ will be constant. We can thus focus on one species, say X_1, which

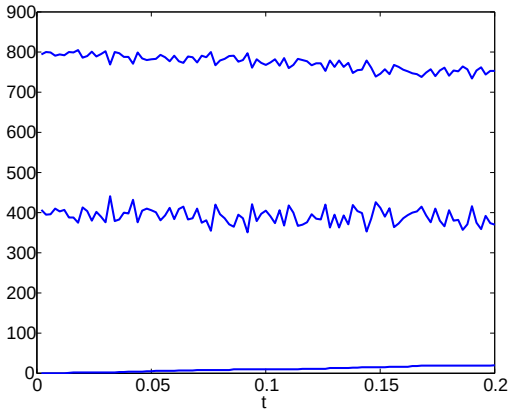

Fig. 5.7. A trajectory for Example 3 simulated by SSA. The upper curve is X_2, the middle curve is X_1, and the lower curve is X_3.

satisfies the (Poisson noise driven) SDE given by

$$dX_1 = -c_2 X_1^2 dt + c_3(X^T - X_1)dt - 2\tilde{N}_1(\boldsymbol{X}, dt) + 2\tilde{N}_2(\boldsymbol{X}, dt). \tag{5.4}$$

The compensated-Poisson random variables satisfy

$$\mathbb{E}\tilde{N}_1(\boldsymbol{X}, dt) = \mathbb{E}\tilde{N}_2(\boldsymbol{X}, dt) = 0,$$
$$\mathrm{Var}\tilde{N}_2(\boldsymbol{X}, dt) = c_3(X^T - X_1)dt/2, \mathrm{Var}\tilde{N}_1(\boldsymbol{X}, dt) = c_2 X_1(X_1 - 1)dt/2 \sim \mathcal{O}(X_1^2)dt.$$

Near equilibrium,

$$c_2 X_1(X_1 - 1)/2 \approx c_3(X^T - X_1)/2,$$

so that $\mathrm{Var}\tilde{N}_2(\boldsymbol{X}, dt) \sim \mathcal{O}(X_1^2)dt$, also. We see from this analysis that the noise terms $\tilde{N}_1(\boldsymbol{X}, dt)$, $\tilde{N}_2(\boldsymbol{X}, dt)$ have quite a large variance at equilibrium if dt is not too small. We are thus not in the situation of trivial invariant measure or mean-square stable systems (for the corresponding Chemical Langevin model). Numerically we found that the strategy developed in [14] (for the choice of m and η) does not work for this system for both the τ-ROCK or the reversed-τ-ROCK method. In order to test the methods, we manually set $\tau = 0.0008$, $m = 3$ and $\eta = 0.7$, and find in this setting the effective step-size is 2.67×10^{-4}, which is only slightly larger than the maximum step-size allowed for the explicit-τ-leaping which is 2.4×10^{-4}. If we want to use large τ, very large m and η are needed. For example for $\tau = 0.01$ the choice of $m = 1000$, and $\eta = 700$ gives a stable integration. But in this case, the effective step-size $\tau/m = 10^{-5}$ is even smaller than step-size allowed for the explicit-τ-leaping method (but the number of random variable generation is significantly smaller for the new methods). Thus, while there is a significant gain for the stochastic effective step-size $\tau_{eff,s}$, there is no gain for the deterministic effective step-size $\tau_{eff,d}$ (see (4.22)).

For this system, the implicit τ-leaping method can give a stable integration even for large τ [15]. But as we mentioned before, important statistical properties such as the variance is not captured for the implicit method. A multiscale explicit-implicit τ-leaping method has been introduced in [15]. Here we mention an alternative strategy that is efficient for such a problem, which is related to the so-called boosting strategy formalized for SDEs in [24] (see also the references therein). In the context of chemical reaction with a fast-slow system as in the Example 3 this strategy works as follows. In a first step we divide the fast and the slow

reactions (here the reactions one and four are slow, while the reactions two and three are fast). Then, first we solve the system keeping the fast forces only (micro-steps); second we solve the system keeping the slow forces only (with initial values given by the result of the micro steps. This procedure is consistent with a modified system where the large variance have been reduced and can be implemented with the τ-leaping method (or τ-ROCK with $m = 1$). Alternatively one could also use the τ-ROCK or the reversed τ-ROCK with reduced noise. More details on this strategy and comparison with existing work will be discussed in a future paper.

6. Conclusion

We discussed new numerical methods for stiff chemical systems driven by Poisson noise. These methods are explicit but nevertheless able to handle efficiently a class of stiff chemical system. They are built upon the ROCK and S-ROCK methods, recently introduced for the numerical solution of stiff ODEs and SDEs. Two different versions of the new methods, the τ-ROCK and the reversed-τ-ROCK have been discussed. The numerical stability and the limit behavior of the new methods have been analyzed on a model problem, the reversible isomerization reaction. We found that both the τ-ROCK and reversed-τ-ROCK methods can capture the mean of the species correctly. While the former method enlarge the variance of the fast species, the latter reduce this variance. This reduction depends on the the step-size Δt, the stage number m and a parameter of the method called the damping coefficient η. These findings seem to suggest that an appropriate combination of the τ-ROCK and the reversed-τ-ROCK methods could lead to better capture the variance. This has to be further explored.

The proposed methods have been tested on three different stiff problems, with different limiting (effective) behavior. The results of the numerical experiments, in accordance with the analysis presented in this paper, show that for systems that are mean square stable, both the τ-ROCK and the modified τ-ROCK methods can use very large step-size while accurately capturing the dynamics of interest. For systems that are not mean square stable, stability is not enough to capture the correct dynamics of the variances of the fast systems which have a non trivial effect on the effective dynamics. This has already been noticed for the S-ROCK methods applied to non-mean square stable stiff SDEs. For such problems, by exploiting the damping property of the reversed-τ-method we show that some stiff non-mean square stable problem can be handled. Finally for non-mean square systems with too large variance, both proposed methods show no improvement compared to the explicit τ-leaping method (which is embedded as a special case in the τ-ROCK or in the modified τ-ROCK methods). The capability of the τ-ROCK and the reversed τ-ROCK methods to be tuned for various situations while keeping the τ-leaping scheme as a special case of the multi-stage schemes, makes these new methods attractive. However, adaptive versions of our methods need to be developed to fully exploit the versatility of the proposed algorithms. This will be addressed in a future work.

Acknowledgement. Hu and Li are supported by the National Science Foundation of China under grant 10871010 and the National Basic Research Program under grant 2005CB321704.

References

[1] A. Arkin, J. Ross and H. McAdams, Stochastic kinetic analysis of developmental pathway bifurcation in phage λ-infected Escherichia coli cells, *Genetics*, **149** (1998), 1633-1648.

[2] M. Elowitz, A. Levine, E. Siggia and P. Swain, Stochastic gene expression in a single cell, *Science*, **297** (2002), 1183-1186.

[3] D. Endy and R. Brent, Modelling cellular behavior, *Nature*, **409** (2001), 391-395.

[4] D. Gillespie, Stochastic simulation of chemical processes, *J. Comput. Phys*, **22** (1976), 403.

[5] D. Gillespie, Exact stochastic simulation of coupled chemical reactions, *J. Phys. Chem.*, **81** (1977), 2340-2361.

[6] D. Gillespie, Approximate accelerated stochastic simulation of chemically reacting systems, *J. Chem. Phys.*, **115** (2001), 1716.

[7] E. Hairer and G. Wanner, Solving Ordinary Differential Equations II: Stiff and Differential-Algebraic Problems, Second Edition, Springer-Verlag, 1996.

[8] A. Abdulle and A. Medovikov, Second order Chebyshev methods based on orthogonal polynomials, *Numer. Math.*, **90**:1 (2001), 1-18.

[9] A. Abdulle, Fourth order Chebyshev methods with recurrence relation, *SIAM J. Sci. Comput.*, **23**:6 (2002), 2042-2055.

[10] P. van der Houwen and B.P. Sommeijer, On the internal stability of explicit m-stage Runge-Kutta methods for large m-values, *Z. angew. Math. Mech*, **60** (1980), 479-485.

[11] V. Lebedev, How to solve stiff systems of differential equations by explicit methods, in *Numerical methods and applications*, Ed. G.I. Marchuk, CRC Press, Boca Raton, Ann Arbor, London, Tokyo (1994), 45-80.

[12] A. Abdulle and S. Cirilli, Stabilized methods for stiff stochastic systems, *C.R. Acad. Sci. Paris, Ser. I*, **345** (2007), 593-598.

[13] A. Abdulle and S. Cirilli, S-ROCK: Chebyshev Methods for Stiff Stochastic Differential Equations, *SIAM J. Sci. Comput.*, **30**:2 (2008), 997-1014.

[14] A. Abdulle and T. Li, Ito S-ROCK methods for stiff stochastic differential equations, *Comm. Math. Sci.*, **6**:4 (2008), 845-868.

[15] M. Rathinam, L. Petzold, Y. Cao and D. Gillespie, Stiffness in stochastic chemically reacting systems: the implicit tau-leaping method, *J. Chem. Phys.*, **119** (2003), 12784.

[16] T. Li, A. Abdulle and E. Weinan, Effectiveness of implicit methods for stiff stochastic differential equations, *Commun. Comput. Phys*, **3**:2 (2008), 295-307.

[17] Y. Cao, L. Petzold, M. Rathinam and D. Gillespie, The numerical stability of leaping methods for stochastic simulation of chemically reacting systems, *J. Chem. Phys.*, **121** (2004), 12169.

[18] Y. Cao, D. Gillespie and L. Petzold, Adaptive explicit-implicit tau-leaping method with automatic tau selection, *J. Chem. Phys.*, **126** (2007), 224101.

[19] T. Tian and K. Burrage Binomial leap methods for simulating stochastic chemical kinetics, *J. Chem. Phys.*, **121** (2004), 10356.

[20] W. E, D. Liu and E. Vanden-Eijnden, Nested stochastic simulation algorithm for chemical kinetic systems with disparate rates, *J. Chem. Phys.*, **123** (2005), 194107.

[21] Y. Cao, L. Petzold and D. Gillespie, The slow-scale stochastic simulation algorithm, *J. Chem. Phys.*, **122** (2005), 14116.

[22] T. Li, Analysis of explicit tau-leaping schemes for simulating chemically reacting systems, *Multiscale. Model. Sim.*, **6** (2007), 417.

[23] N. Van Kampen, Stochastic Processes in Physics and Chemistry, Elsevier, Amsterdam, The Netherlands, 1992.

[24] E. Vanden-Eijnden, On HMM-like integrators and projective integration methods for systems with multiple time scales, *Comm. Math. Sci.,* **5** (2007), 495.